Geomechanics and Engineering, *Vol. 41, No. 6 (2025) 583-596*
https://doi.org/10.12989/gae.2025.41.6.583

Analysis of single pile in two-layered soil subjected to uplift load

Sudip Basack*[1,2], Meshel Q Alkahtani[3a] and Saiful Islam[3b]

[1]*Principal, Regent Education and Research Foundation, Affiliated: MAKA University of Technology, Kolkata, India*
[2]*Department of Civil Engineering, Graphic Era Deemed to be University, Dehradun, Uttarakhand, India*
[3]*Department of Civil Engineering, College of Engineering, King Khalid University, Abha, Saudi Arabia*

(*Received February 12, 2025, Revised June 1, 2025, Accepted June 7, 2025*)

Abstract. Studies on uplift piles in layered soil have been insufficient. This study aimed to develop an analytical model to predict the limit state performance of single pile in two-layered soil under uplift load. Appropriate mathematical correlations have been derived for uplift capacity and limiting displacement of piles considering limit state analysis. Validation of the model by comparison with available experimental and theoretical results ensured its accuracy. The model has been applied to conduct parametric studies and develop design curves for uplift pile design considering safety and serviceability criteria. A typical design example has also been illustrated. From the entire study, relevant conclusions are drawn.

Keywords: cohesionless soil; cohesive soil; layered soil; single pile; uplift load

1. Introduction

Pile foundations are sometimes subjected to uplift loading. Piles supporting offshore and onshore structures, transmission towers, bridges, high-rise buildings, etc., are subjected to pullout load due to the action of wind, wave, traffic movement, etc., initiated by overturning moment, hydrostatic pressure or seismic loading (Zhu *et al*. 2014, Park and Lee 2021). These piles resist the imparted uplift load due to skin friction in case of floating piles, unless the piles are socketed at the tip wherein the majority of pullout is resisted by base restraint (Li *et al.* 2021, Fang *et al.* 2023). The pullout loads are also resisted by bearing pressures in cases of under-reamed piles and helical piles (Kumar *et al*. 2020, Karami *et al*. 2023, 2024). The design requirements for uplift piles are to provide adequate factor of safety against ultimate failure and acceptable upward displacement at pile head (Alawneh 1999, Lee *et al*. 2009).

An extensive review of the existing contributions reveal that several studies have been conducted on uplift piles in uniform soil, including analytical (Su *et al*. 2014, Zhang *et al.* 2018, Liu *et al.* 2023) and numerical (Hong-nan *et al*. 2015, Kranthikumar *et al*. 2016, Basack *et al*. 2025, Saleh *et al.* 2025) modelling, laboratory model study (Reddy and Ayothiraman 2015, Gui *et al.* 2021, Dong *et al.* 2023, Nour El-Deen *et al*. 2025, Raju and Lakshmi 2025) and field-based investigations (Xu *et al.* 2014, Yu *et al*. 2023). Although limited past studies were conducted on uplift piles in layered soil (Pusadkar and Ghormode 2015, Ashour and Abbas 2020), a comprehensive analysis on single piles in layered soil under pullout load together considering safety and serviceability criteria, with development of appropriate design methodology is yet to be carried out. The current study is aimed towards developing an analytical model on uplift pile performance in two-layered soil under limit state condition, so as to derive appropriate.

∗Corresponding author, Professor
E-mail: basackdrs@hotmail.com
[a]Professor
[b]Lecturer

2. Problem identification

The idealized problem has been depicted in Fig. 1, wherein a single, vertical, floating pile having circular cross section of diameter D and length L is embedded in a two-layered soil, and the depth of upper layer being z_1. When subjected to an uplift load of P, vertically downward shear stress is induced on the pile surface; at a depth of z on the pile surface (point 'A'), the shear stress is denoted as τ_z.

3. Theoretical analysis

The mathematical derivations involved in development of the analytical solution are described in this section.

3.1 Assumptions

The analytical model is based on the following assumptions:

(i) The layer-2 is semi-infinite.
(ii) The pile is subjected to pure axial tension without any other load.
(iii) No residual stress exists in the soil due to pile installation.
(iv) The pile base is not restraint against upward displacement.

The pile is assumed to be elastic-perfectly plastic, while the stress-strain correlation of soil is hyperbolic with a reduction factor of R_f. For most soils, R_f varies from 0.8 to

ISSN: 2005-307X (Print), 2092-6219 (Online)

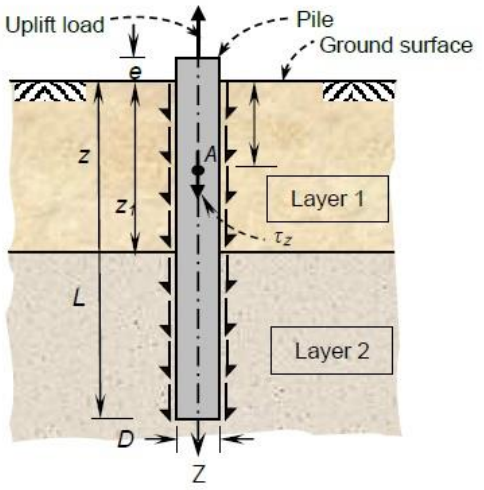

Fig. 1 The idealized problem

1.0 (Duncan and Chang 1970, Randolph 2003).

3.2 Ultimate uplift capacity

As the uplift load *P* is gradually increased, the failure condition is attained when pile-soil slippage occurs for the entire pile-soil interface, or the pile material itself fails under tensile stress, whichever is earlier (Basack *et al.* 2025). Mathematically

$$P_u = Min\left\{P_u^s, P_u^p\right\} + W_p \tag{1}$$

where, P_u is the ultimate uplift capacity of the pile, P_u^s and P_u^p are the uplift loads corresponding to complete pile-soil interface slippage, and tension failure of the pile material, respectively, and W_p is the self-weight of pile.

In case of cylindrical pile, the self-weight is given as

$$W_p = \frac{\pi}{4}D^2(L+e)\gamma_p \tag{2}$$

where, γ_p is the unit weight of pile material. Based on limit state analysis, the value of P_u^scan be written by (Poulos and Davis 1980, Basack and Khabbaz 2024)

$$P_u^s = \int_0^L \pi D\tau_z^u \, dz \tag{3}$$

where, τ_z^u is the yield shear stress of soil at the pile-soil interface, given by (Basack and Sen 2014)

$$\begin{aligned} \tau_z^u &= \alpha(c_u^0 + \eta_c z) && \text{[for clay]} \\ \tau_z^u &= K_s\sigma'_{v_z}\tan\delta_s && \text{[for sand]} \end{aligned} \tag{4}$$

where, α is the interface adhesion factor, c_u^0 is the unit cohesion of clay at the ground surface, η_c is the rate of increase of unit cohesion with depth, K_s is the in-situ earth pressure coefficient, σ'_{v_z} is effective vertical overburden stress in soil at depth z, and δ_s is interface friction angle.

The value of P_u^p, on the other hand, has been derived from the conventional theory of solid mechanics (Bertram and Glüge 2015), given as

$$P_u^p = \frac{\pi}{4}D^2\sigma_p^u \tag{5}$$

where, σ_p^u is the limiting stress in the pile material at tensile failure.

Analysis has been performed separately for clay overlying sand and vice versa, as detailed below.

3.2.1 Clay overlying sand

In this case, the soil layers numbered as 1 and 2 (see Fig. 1) are considered as clay and sand respectively. The groundwater table has been assumed to be situated at ground surface. The Eq. (3) can be re-written as

$$P_u^s = \pi D\left[\int_0^{z_1} \alpha(c_u^0 + \eta_c z)\, dz + \int_{z_1}^{L} K_s\{\gamma'_c z_1 + \gamma'_s(z - z_1)\}\tan\delta_s \, dz\right] \tag{6}$$

where, γ'_c and γ'_s are the effective unit weights of clay and sand, respectively.

Carrying out the above integration, the following expression has been obtained

$$P_u^s = \pi D\left[\alpha\left(c_u^0 z_1 + \eta_c\frac{{z_1}^2}{2}\right) + K_s\tan\delta_s\left\{\gamma'_c z_1(L - z_1) + \gamma'_s\frac{(L-z_1)^2}{2}\right\}\right] \tag{7}$$

3.2.2 Sand overlying clay

In this case, the soil layers described in above (section 3.2.1) have been reversed and the groundwater table has been chosen to be situated at ground surface. Here, the Eq. (3) can be re-written as,

$$P_u^s = \pi D\left[\int_0^{z_1} K_s\tan\delta_s\,\gamma'_s z\, dz + \int_{z_1}^{L}\alpha\left(c_u^{z_1} + \eta_c z\right)dz\right] \tag{8}$$

where, γ'_c and γ'_s are the effective unit weights of clay and sand, respectively.

Carrying out the above integration, the following expression has been obtained

$$P_u^s = \pi D\left[K_s\tan\delta_s\,\gamma'_s\frac{{z_1}^2}{2} + \alpha\left\{c_u^{z_1}(L - z_1) + \eta_c\frac{(L-z_1)^2}{2}\right\}\right] \tag{9}$$

Logically, tension failure is likely to take place whenever $P_u^p/P_u^s > 1$. For sufficiently long piles, failure of pile material in tension usually occurs prior to pile-soil slippage (Phanikanth *et al.* 2010, Basack and Nimbalkar 2017, Basack *et al*. 2025).

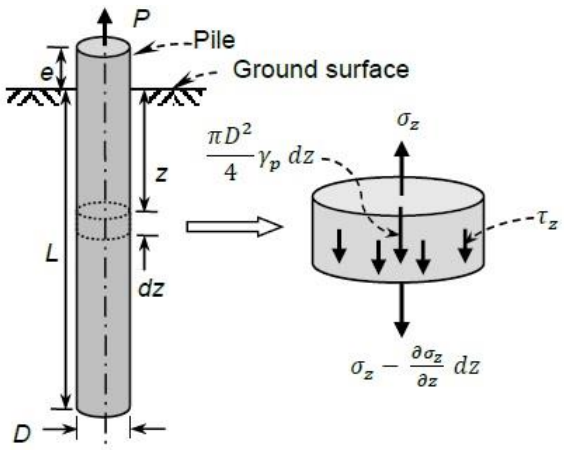

Fig. 2 Cylindrical pile element with stress components

3.3 Maximum uplift displacement

Considering an infinitesimal and cylindrical pile element shown in Fig. 2, the vertical equilibrium condition of the element yields the following expression

$$\frac{\partial \sigma_z}{\partial z} = \frac{4\tau_z}{D} + \gamma_p \tag{10}$$

where, σ_z is the tensile stress on a pile cross section at a depth of z, τ_z is the interface shear stress at a depth of z and γ_p is the unit weight of pile.

From classical theory of solid mechanics (Bertram and Glüge 2015), the elongation of the pile element is given by

$$d\rho_z = \left(\sigma_z / E_p\right) dz \tag{11}$$

where, ρ_z is the elongation of the pile element and E_p is the Young's modulus of the pile. Differentiating Eq. (11) with respect to z and using Eq (10), the following correlation is obtained

$$\frac{\partial^2 \rho_z}{\partial z^2} = \frac{1}{E_p}\left(\frac{4\tau_z}{D} + \gamma_p\right) \tag{12}$$

Using Eq (12), the net upward displacement of the pile head is therefore given by

$$\rho_h = \frac{P(L+e)}{(\pi D^2/4)E_p} + \rho_b - \frac{1}{E_p}\int_0^L \left[\int_0^L \left(\frac{4\tau_z}{D} + \gamma_p\right) dz\right] dz \tag{13}$$

where, ρ_b is the upward displacement at the pile base. At pre-slippage stage, ρ_b is given as (Randolph and Wroth 1978, FHWA 2006)

$$\rho_b = \frac{\tau_b}{(2G_s^b/D)} \ln\left[\frac{5L(1-\mu_s)}{D\left(G_s^b/G_s^{L/2}\right)}\right] \tag{14}$$

where, τ_b is the interface shear stress at pile base level, μ_s is the Poisson's ratio of soil, and G_s^b and $G_s^{L/2}$ are the secant modulii of soil at pile base and at $z = L/2$. After hyperbolic soil model, the following correlation holds good

$$G_s^z = \left(G_t^0 + \eta_g z\right)\left[1 - R_f(\tau_z/\tau_z^u)\right] \tag{15}$$

where, G_s^z is the secant modulus of soil at a depth of z, G_t^0 is the initial tangent modulus of soil at $z = 0$ and η_g is the rate of increase of initial tangent modulus of soil with z.

As observed from previous studies, the interface shear stress is maximum at the ground surface and minimum at the base. Thus, pile-soil slippage is commenced from the ground surface and increasingly progresses downward, as the magnitude of the upward load P is gradually increased (Ashour and Abbas 2020, Basack *et al.* 2025). At the onset of uplift pile failure by interface slippage, $\tau_b = \tau_b^u$ and Eq. (14) is still applicable at the pile-base. Therefore, the upward displacement of the pile head has been derived from Eqs. (12)-(14) which is given as

$$\begin{aligned}\rho_h^u &= \frac{P_u^s(L+e)}{(\pi D^2/4)E_p} + \frac{\tau_b^u}{\left[2G_t^b(1-R_f)/D\right]} \ln\left[\frac{5L(1-\nu_s)}{D\left(G_t^b/G_t^{L/2}\right)}\right] \\ &\quad - \frac{1}{E_p}\int_0^L \left[\int_0^L \left(\frac{4\tau_z^u}{D} + \gamma_p\right) dz\right] dz\end{aligned} \tag{16}$$

where, τ_b^u is the peak shear stress at base, ν_s is the Poisson's ratio of soil, and G_t^b and $G_t^{L/2}$ are the initial tangent moduli of soil at $z = L$ and $L/2$, respectively.

For two-layered soil, appropriate correlations for peak uplift displacement of pile head have been derived by carrying out the integration of Eq. (16) above, as described below.

3.3.1 Clay overlying sand

In this case, the integration in Eq. (16) has been conducted and the expression is given by

$$\rho_h^u = \rho_1 + \rho_2 - \rho_3 \tag{17}$$

where, the components ρ_1, ρ_2, and ρ_3 are given as

$$\rho_1 = \frac{P_u^s(L+e)}{(\pi D^2/4)E_p} \tag{18}$$

$$\rho_2 = \frac{K_s\{\gamma_c' z_1 + \gamma_s'(L-z_1)\}\tan\delta_s}{\left[2G_t^b(1-R_f)/D\right]} \ln\left[\frac{5L(1-\nu_s)}{D\left(G_t^b/G_t^{L/2}\right)}\right] \tag{19}$$

$$\begin{aligned}\rho_3 = \frac{L^2\gamma_p}{2E_p} + \frac{4}{DE_p}\Bigg[\alpha\left(c_u^0\frac{{z_1}^2}{2} + \eta_c\frac{z_1^3}{6}\right) \\ + K_s\tan\delta_s\left\{\gamma_c' z_1\frac{(L^2-{z_1}^2)}{2} \right. \\ \left. + \gamma_s'\frac{(L-z_1)^3}{6}\right\}\Bigg]\end{aligned} \tag{20}$$

Idealizing the soil stiffness to increase linearly with depth, the secant moduli of soil given in the above equations may be expressed as follows

$$G_t^b = G_{t_2}^0 + \eta_{g_2}(L - z_1) \tag{21a}$$

$$G_t^{L/2} = G_{t_1}^0 + \eta_{g_1}\frac{L}{2} \qquad (\text{If } z_l > L/2) \tag{21b}$$

$$= G_{t_2}^{z_1} + \eta_{g_2}(L/2 - z_1) \qquad (\text{If } z_1 < L/2)$$

$$= \frac{G_{t_1}^0 + \eta_{g_1}\frac{L}{2} + G_{t_2}^{z_1}}{2} \qquad (\text{If } z_1 = L/2)$$

where, $G_{t_1}^0$, $G_{t_2}^{z_1}$, η_{g_1} and η_{g_2} are the soil parameters G_t^0 and η_g relevant to layers 1 and 2, respectively.

3.3.2 Sand overlying clay

In this case, the maximum uplift pile head displacement is given by Eq. (17) above. While ρ_1 is obtained by Eq. (18), ρ_2 and ρ_3 are given as

$$\rho_2 = \frac{\alpha\left(c_u^{z_1} + \eta_c z_1\right)}{\left[2G_t^b\left(1 - R_f\right)/D\right]} \ln\left[\frac{5L(1-\nu_s)}{D\left(G_t^b/G_t^{L/2}\right)}\right] \qquad (22)$$

$$\rho_3 = \frac{L^2\gamma_p}{2E_p} + \frac{4}{DE_p}\left[K_s \tan\delta_s\left(\gamma_s' \frac{z_1^3}{6}\right) + \alpha\left\{c_u^{z_1}\frac{(L-z_1)^2}{2} + \eta_c\frac{(L-z_1)^3}{6}\right\}\right] \qquad (23)$$

The shear moduli G_t^b and $G_t^{L/2}$ may be obtained from Eqs. (20) and (21), respectively.

4. Validation

To verify the accuracy of the analytical model and the formulations developed above have been compared with available experimental data and results from existing solutions.

Carvalho and Albuquerque (2013) carried out a set of full-scale field based investigations at Brazil on concrete bored piles embedded in layered sandy soil consisting of different upper and lower sandy soil layers, each having 6 m thickness. The ground water table was located at a depth of 10 m below ground surface. The single, vertical concrete pile were of length 10 m and diameter of 0.35 m, 0.4 m and 0.5 m. The soil parameters and pile geometry are taken in accordance with those reported by Carvalho and Albuquerque (2013) along with few reasonably assumed parameters, and presented in Table 1. The initial tangent modulus of the soil layers were estimated from the reported field values of standard penetration tests. The comparison of analytical values with field test data is depicted in Fig. 3.

The analytical values of ultimate uplift capacity of the piles have been evaluated utilizing Eqs. (1) to (5). It has been observed from analysis that the pile-soil slippage occurred prior to pile material failure in tension, based on the chosen value of σ_p.

The analytical limiting upward pile head displacement has been evaluated using Eq. (16). Since both the layers are sandy, the Eqs. (19), (20) and (22) are not directly applicable in these cases.

The field values of ultimate uplift capacity have been estimated from the in-situ load-displacement responses and using double-tangent technique (Basack *et al.* 2022). The limiting pile displacement was chosen at the point where the field load-displacement curves started exhibiting linear variation, based on the analysis of Das and Seeley (1982) and Narasimha Rao and Prasad (1993).

Table 1 Input parameters for analysis after Carvalho and Albuquerque (2013)

Material	Parameter	Value	
		Layer-1	Layer-2
Soil	Thickness (m)	6	12
	Bulk unit weight, γ_s (kN/m^3)	16.3	18.9
	Initial shear modulus of soil, G_t^0 (MPa)	28 [a]	40 [a]
	Depth-rate of increase of shear modulus, η_g (MPa/m)	0	0
	Poisson's ratio, ν_s	0.3 [b]	0.3 [b]
	Undrained cohesion at ground surface, c_u^0 (kPa)	0	0
	Rate of increase of cohesion with depth, η_c (kPa/m)	0	0
	Effective friction angle, ϕ' (^{0})	30^o	23^o
	Stress reduction factor, R_f	0.8 [c]	0.8 [c]
	In-situ earth pressure coefficient, K_s	0.5 [d]	0.609 [d]
	Interface friction angle, δ_s	1.0 ϕ' [d]	1.0 ϕ' [d]
Piles	Diameter, D (m)	0.35, 0.4, 0.5	
	Embedded length, L (m)	10	
	Unit weight of pile material, γ_p (kN/m^3)	25 [e]	
	Young's modulus, E_p (GPa)	3 [e]	
	Plastic stress in tension, σ_p (MPa)	500 [f]	

Data assumed after: [a]Anbazhagan *et al*. (2012, 2021); [b]Ashour and Abbas (2020), [c] Randolph (2003), [d] Awad-Alla *et al.* (2009), Kulhawy *et al.* (1983), Kulhawy (1991), [e]McCormac and Brown (2015), [f]Moghadam and Izadifard (2021)

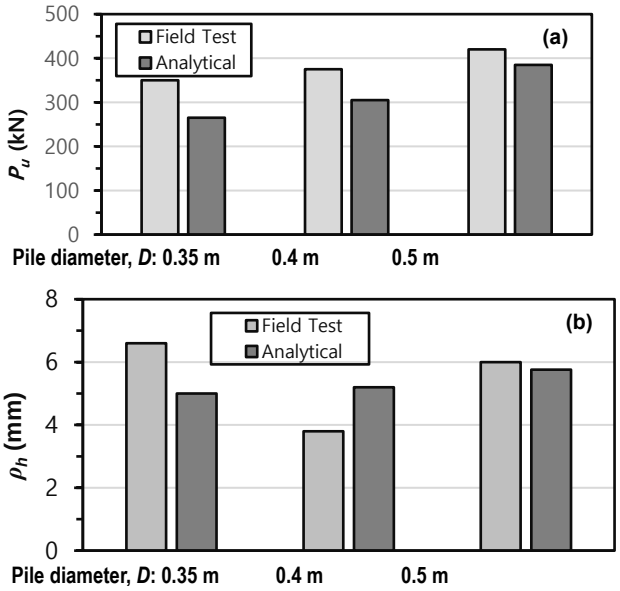

Fig. 3 Comparison of analytical results with field test data of Carvalho and Albuquerque (2013): (a) Ultimate uplift capacity, and (b) Limiting upward displacement

Table 2 Input parameters for analysis after Massoudi and Bell (2017)

Material	Parameter	Value		
		Layer1	Layer3	Layer2
Soil	Thickness (m)	1.83	4.11	14.0
	Unit weight (kN/m^3)	19	18	19.5
	Initial shear modulus of soil, G_t^0 (MPa)	NR	NR	24.55
	Rate of increase of shear modulus with depth, η_g (MPa/m)	NR	NR	6
	Poisson's ratio, v_s	0.5[a]	0.3[a]	0.5[a]
	Undrained cohesion at surface, c_u^0 (kPa)	70	0	190
	Rate of increase of cohesion with depth, η_c (kPa/m)	0	0	37.86
	Adhesion factor, α	0.55[b]	NR	0.35[b]
	Effective friction angle, ϕ' (^{0})	0	34	0
	Stress reduction factor, R_f	0.8 [c]	0.8 [c]	0.8 [c]
	In-situ earth pressure coefficient, K_s	NR	0.309[d]	NR
	Interface friction angle, δ_s	NR	0.9ϕ' [d]	NR
Piles	Diameter, D (m)		0.457	
	Embedded length, L (m)		16.76	
	Unit weight of pile material, γ_p (kN/m^3)		25 [e]	
	Young's modulus, E_p (GPa)		3 [e]	
	Plastic stress in tension, σ_p (MPa)		500 [f]	

Notes: (1) NR: Not required. (2) Data assumed after: [a]Ashour and Abbas (2020), [b]Cherubini and Vessia (2007), [c] Randolph (2003), [d]Awad-Alla *et al.* (2009), Kulhawy *et al.* (1983), Kulhawy (1991), [e]McCormac and Brown (2015), [f] Moghadam and Izadifard (2021)

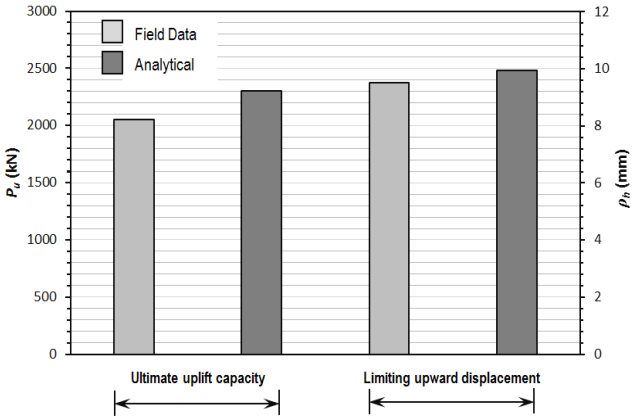

Fig. 4 Comparison of analytical results with field data of Massoudi and Bell (2017)

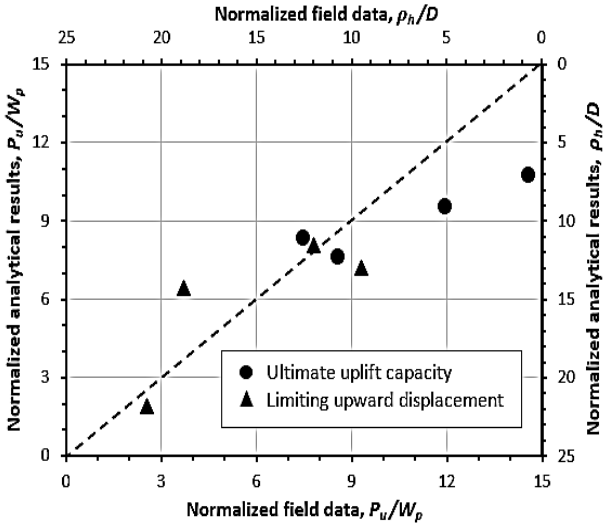

Fig. 5 Comparative study of normalized analytical and field test results

As observed from Fig. 3, the average variation has been about 21%, with the analytical capacities on the lower side. In reality, the presence of silt and clay in the sandy soil layers exhibited minor cohesion, as reported by Carvalho and Albuquerque (2013), which have not been taken into account in the analysis. Since no direct field data pertaining to the soil shear moduli is available, their assumed values have as well attributed to the deviation of pile displacement.

Massoudi and Bell (2017) conducted a series of field tests at Austin, Texas, USA, on uplift performance of auger bored cast in-situ concrete piles embedded in three layered soil comprising of upper clayey layer, middle sandy soil and bottom stiff clay layer. The groundwater table was situated at a depth of 2.13 m below the ground surface. The soil and pile parameters were chosen based on the reported in-situ values, together with few assumed value, as presented in Table 2. The initial tangent moduli of soil have been assumed from the available values of soil strength and ε_{50} (i.e., strain at 50% stress level) based on the analysis given by Ashour and Abbas (2020).

As observed, the deviation of analytical results with the field-based data have been about 12% and 4.5% for ultimate uplift capacity and limiting upward displacement respectively, the analytical results being on the higher side. Such minor deviations possibly took place due to assumed values of few soil and pile parameters including α, R_f, K_s, δ_s, E_p, etc. In the analysis, the pile-soil has been found to occur prior to tension failure of pile material.

For comparative study, the ultimate uplift capacity and the limiting upward pile displacement have been normalized by the self-weight of pile (W_p) and pile diameter (D), respectively. The analytical values of these non-dimensionalized parameters have been plotted against the relevant field values, as shown in Fig. 5. It has been observed that the data point are close to the 45^o line, indicating accuracy of the analytical formulations developed.

5. Parametric studies

The analytical solution and the formulations have been

Table 3 Input soil and pile data for parametric study

Material	Parameter	Value	
		Clay	Sand
Soil	Unit weight (kN/m^3)	18	20
	Initial shear modulus of soil, G_t^0 (MPa)	30-50	0
	Rate of increase of shear modulus with depth, η_g (MPa/m)	0.3 – 0.5	3 (ϕ'=20°) 5 (ϕ'=30°) 7 (ϕ'=40°)
	Poisson's ratio, v_s	0.5 [a]	0.3 [a]
	Undrained cohesion at ground surface, c_u^0 (kPa)	30-50	0
	Rate of increase of cohesion with depth, η_c (kPa/m)	3-5	0
	Adhesion factor, α	0.5 [b]	-
	Effective friction angle, ϕ' (^{0})	0	20° – 40°
	Stress reduction factor, R_f	0.9 [c]	0.9 [c]
	In-situ earth pressure coefficient, K_s	-	1-sin ϕ' [d]
	Interface friction angle, δ_s	1.0 ϕ' [d]	1.0 ϕ' [d]
Piles	Diameter, D (m)	0.33, 0.5, 1.0	
	Embedded length, L (m)	10	
	Unit weight of pile material, γ_p (kN/m^3)	25 [e]	
	Young's modulus, E_p (GPa)	3 [e]	
	Plastic stress in tension, σ_p (MPa)	500 [f]	

Data assumed after: [a] Ashour and Abbas (2020), [b] Cherubini and Vessia (2007), [c] Randolph (2003), Basack and Khabbaz (2024), [d] Awad-Alla *et al.* (2009), Kulhawy *et al.* (1983), Kulhawy (1991), [e] McCormac and Brown (2015), [f] Moghadam and Izadifard (2021)

utilized to perform an extensive parametric study and develop appropriate design recommendations. A vertical concrete pile has been assumed to be embedded in a two-layered soil, taking the data pertaining to a similar case study conducted earlier (Basack and Hadi 2024, Basack and Sen 2014). The depth of embedment of pile has been kept at a constant value of L = 10 m, while the pile diameter D has been varied 0.33 m, 0.5 m and 1 m, so that the L/D ratio altered as 30, 20 and 10, respectively. The pile head and the ground water table has been assumed at the ground surface. The layer thickness ratio z_1/L and the soil strength and stiffness have been varied in specified ranges and appropriate results relevant to the ultimate uplift capacity and limiting displacement have been evaluated. The soil and pile input parameters are presented in Table 3.

For the convenience of conducting the repetitive analytical computations, a user-friendly computer program APUL has been developed in Fortran 90 language. Separate subroutines were written for ultimate uplift pile capacity and the limiting upward pile head displacement, as well as for clay overlying sand and vice versa. The flowchart of the program is portrayed in Fig. 6.

Analytical results pertaining to clay overlying sand and vice versa have been separately presented herein below sequentially.

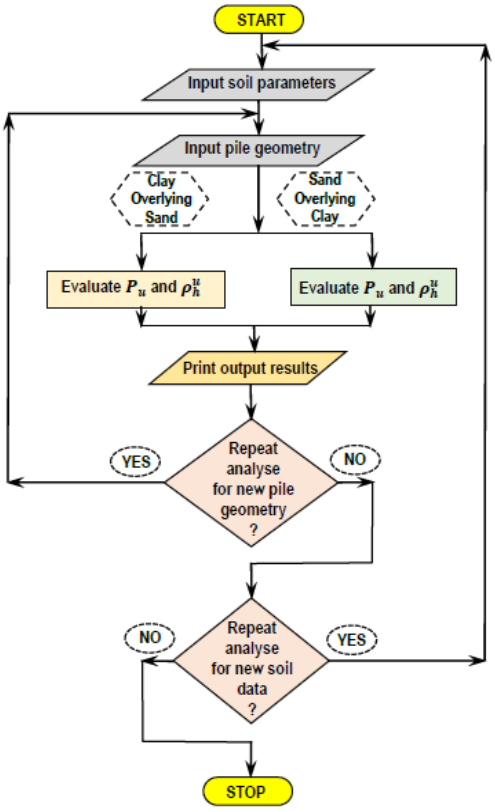

Fig. 6 Flowchart of the computer program APUL

5.1 Ultimate uplift capacity

Using the developed correlation, variation in the ultimate uplift pile capacity for various soil parameters, pile geometry and layer thickness ration (z_1/L) has been studied, using the developed correlations. Separate presentations for clay overlying sand and vice versa has been made below.

5.1.1 Clay overlying sand

In the case of clay overlying sand, the correlation used are Eqs. (6) and (7). It has been noted that failure by a complete pile-soil slippage took place prior to tensile failure of pile material. The ultimate uplift pile capacity has been normalized by $\alpha c_u^0 D^2$. The values of normalized capacity have been plotted against the soil layer thickness ration z_1/L, for different values of L/D ratio and soil strength c_u^0, η_c and ϕ', as depicted in Fig. 7. The curves have been curvilinear with ascending slopes. For the chosen values of L/D ratio, the normalized capacity initially decreased to minimum values and thereafter increased. The value of z_1/L at which the minimum capacity was attained was found to be decreased with increasing soil strength. This plot may be utilized to evaluate the ultimate uplift capacity of the pile at the desired soil thickness ratio for the desired L/D ratio and soil strengths.

5.1.2 Sand overlying clay

In the case where the upper layer is sand while the lower layer is clay, Eqs. (8) and (9) have been applied. For all the

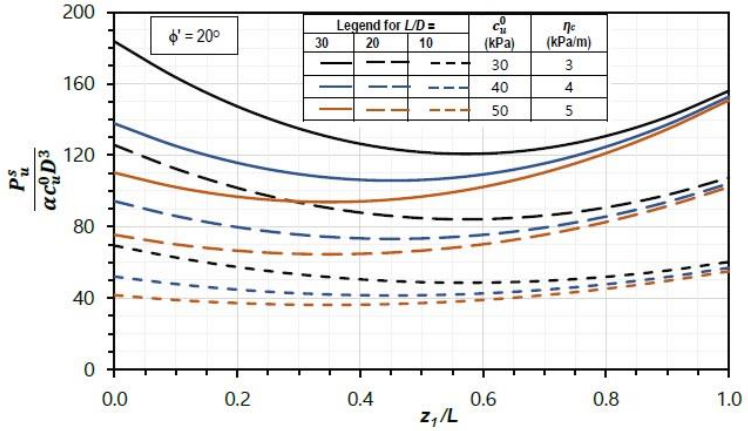

(a) ϕ' = 20°

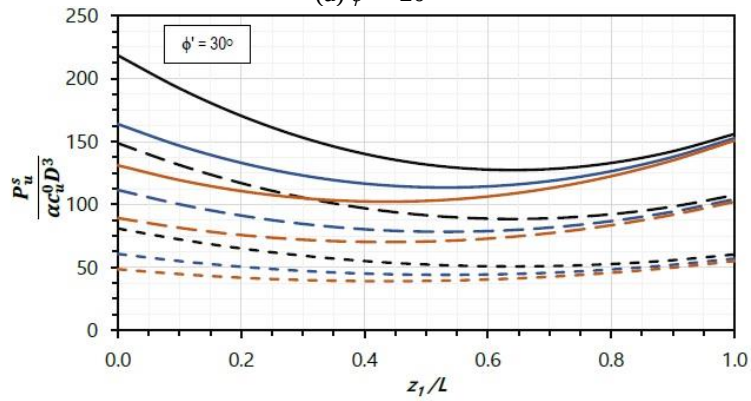

(b) ϕ' = 30°

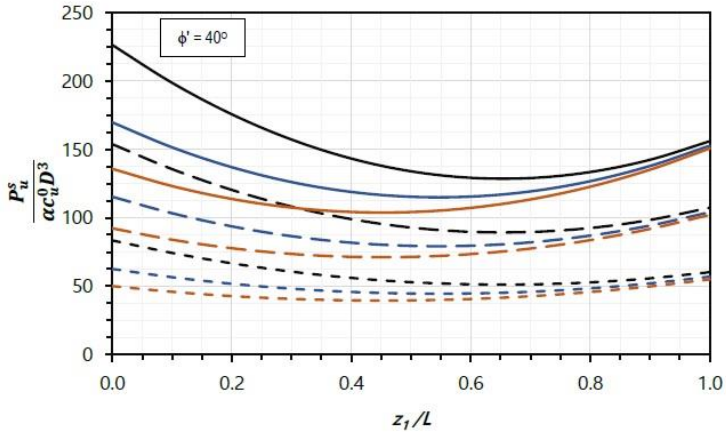

(c) ϕ' = 40°

Fig. 7 Variation of normalized uplift pile capacity with z_1/L for clay overlying sand

soil and pile parameters, pile-soil slippage occurred prior to tensile failure of pile.

The variation of ultimate uplift capacity of the piles with the soil layer thickness ratio z_1/L have been plotted in Fig. 8 for different soil strengths of sand and clay. In order to conduct a generalized study, the ultimate uplift capacity has been normalized by the quantity $\alpha K_s tan\ \delta_s \gamma_s' D^3$.

For the chosen ranges of soil parameters, pile geometry, and soil layer thickness, the normalized ultimate uplift pile capacity was observed to vary from 3 x 10^3 to 50 x 10^3. The curves were found to be curvilinear with ascending slopes. With increase in thickness ratio z_1/L, the normalized capacity was observed to initially decrease up to a minimum value, and thereafter increased progressively. The value of z_1/L at which this minimization took place increased with ascending soil strengths of both the layers.

5.2 Limiting uward ple dsplacement

Apart from pile capacity, upward displacement of the pile head due to pullout load is an essential parameter to

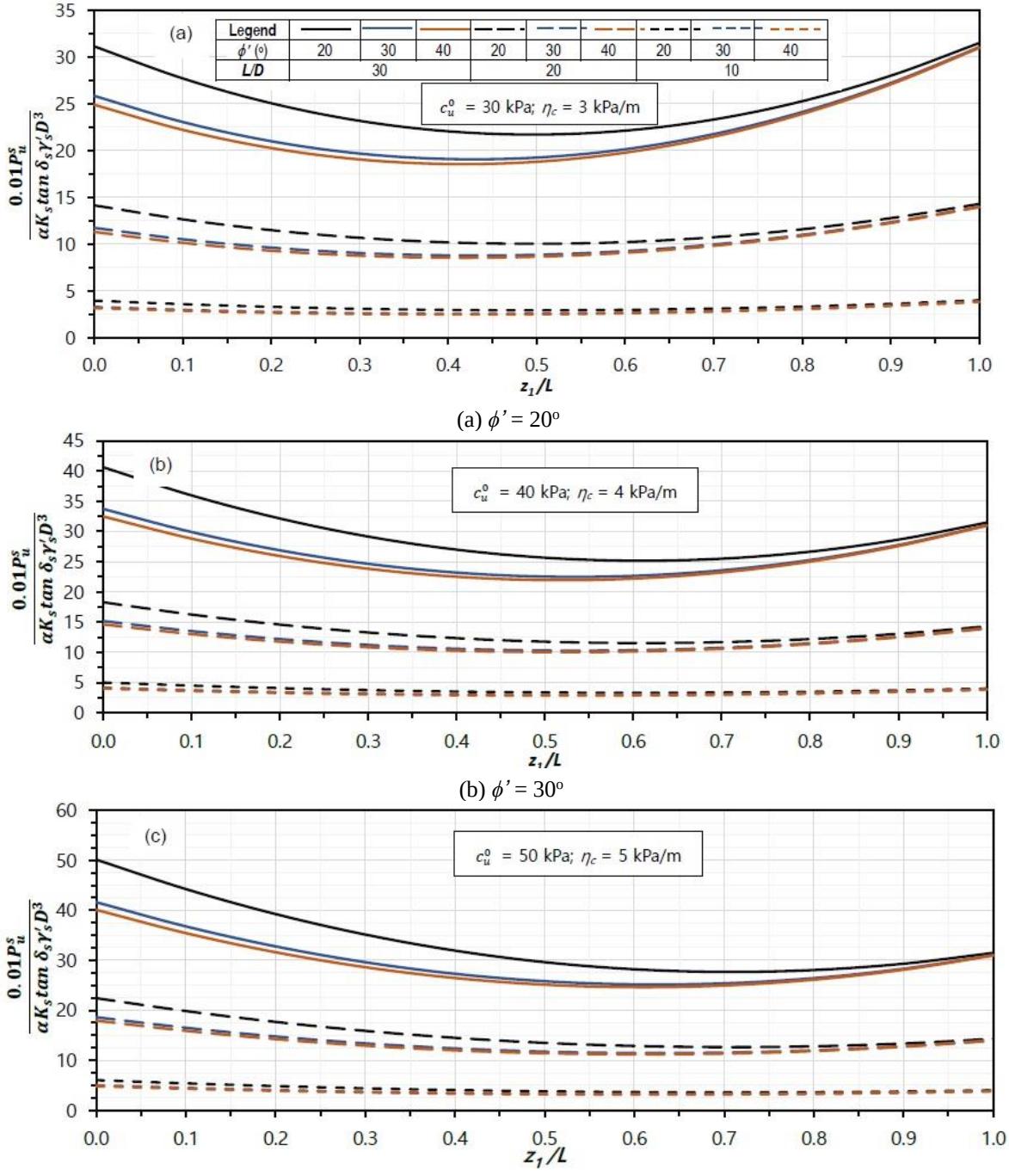

(a) ϕ' = 20°

(b) ϕ' = 30°

(c) ϕ' = 40°

Fig. 8 Variation of normalized uplift pile capacity with z_1/L in case of sand overlying clay for bottom clay layer strength (c_u^0 and η_c): (a) 30 kPa & 3 kPa/m, (b) 40 kPa & 4 kPa/m, and (c) 50 kPa & 5 kPa/m

ensure the serviceability criteria. In this section, the variation of limiting upward pile displacement with respect to soil thickness ratio has been studied.

5.2.1 Clay oerlying snd

In this case, Eqs. (17) to (20) are applied. The variation of normalized pile head displacement ρ_h/D with soil thickness ratio z_1/L has been plotted in Fig. 9 for various soil parameters and pile geometry. With the chosen values of soil parameters and pile geometry, the magnitude of normalized pile head displacement was found to vary from 1% to 2.2%. As observed, the variations have been curvilinear with the magnitude of curvature progressively decreased with increasing strength and stiffness of upper clay layer. In case of L/D = 30, the value of ρ_h/D was found to decrease with initial values of z_1/L up to a minimum magnitude and thereafter increased. On the other hand, for L/D of 10 and 20, ρ_h/D decreased continuously.

5.2.2 Sand overlying clay

Herein, the correlations in Eqs. (17), (18), (22) and (23) have been applicable. For different values of strength and

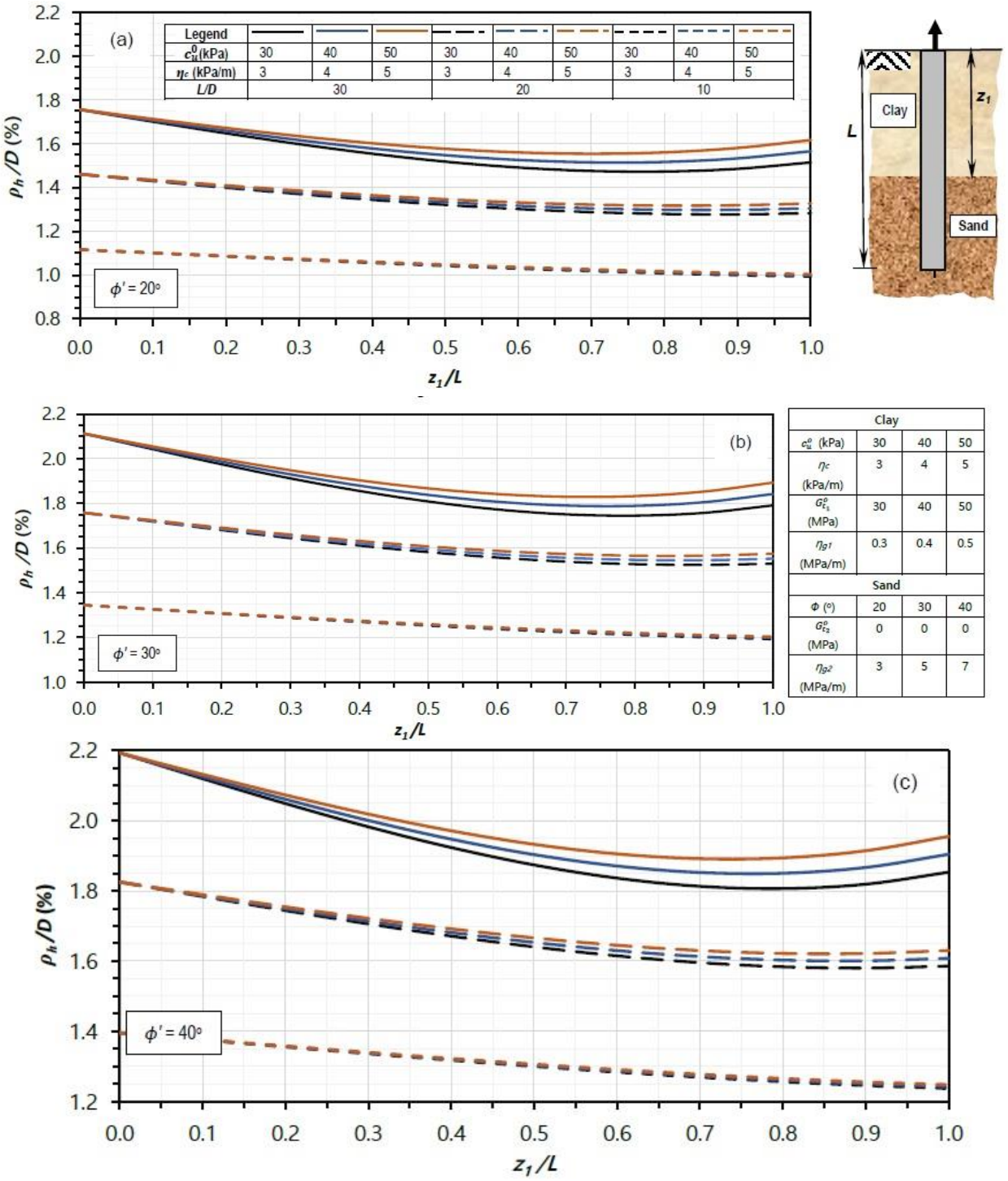

Fig. 9 Variation of normalized pile head upward displacement with z_1 /L in case of clay overlying sand, for effective friction angle of sand (ϕ') as: (a) 20°, (b) 30°, and (c) 40°

stiffness of the sand and clay layers, the variation of normalized pile head displacement ρ_h/D with soil thickness ratio z_1/L has been plotted in Fig. 10 for various L/D ratios. With the chosen values of soil parameters and pile geometry, the magnitudes of displacement was observed to vary in the range of $0.38\% \leq \rho_h/D \leq 1.35\%$, as the layer thickness ratio varied from 0 to 1.

The pattern of variation of normalized pile head upward displacement (ρ_h/D) was observed to be increasing with soil layer thickness (z_1 /D) in a fairly linear trend. The magnitude of displacement was found to be reduced with ascending soil stiffness. For higher stiffness of upper sand layer, the curves almost coincided for $L/D > 0.6$. Furthermore, variation of stiffness of bottom clay layer did not produced notable variation in the displacement magnitudes. For lowest value of stiffness of upper sand layer, the curves intersected at z_1 /L = 0.7.

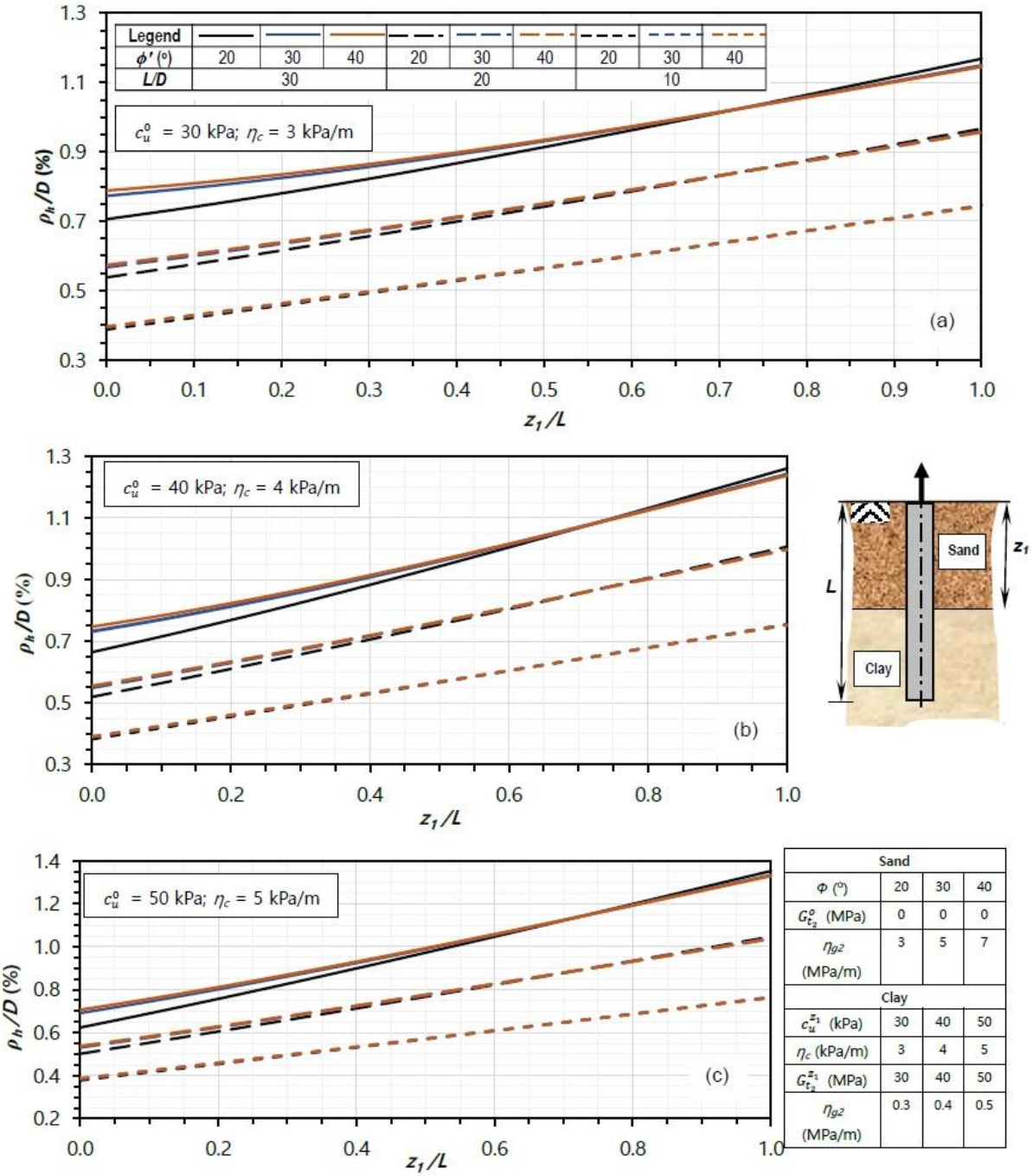

Sand			
Φ (°)	20	30	40
$G_{t_2}^o$ (MPa)	0	0	0
η_{g2} (MPa/m)	3	5	7
Clay			
$c_u^{z_1}$ (kPa)	30	40	50
η_c (kPa/m)	3	4	5
$G_{t_2}^{z_1}$ (MPa)	30	40	50
η_{g2} (MPa/m)	0.3	0.4	0.5

Fig. 10 Variation of normalized pile head upward displacement with z_1/L in case of sand overlying clay, for bottom clay layer strength ($c_u^0$and η_c): (a) 30 kPa & 3 kPa/m, (b) 40 kPa & 4 kPa/m, and (c) 50 kPa & 5 kPa/m

5.3 Analysis and interpretations

The appropriate magnitude of uplift pile capacity in layered soil largely depends upon the relative shear strengths of the soil layers (Wang 2022). Ascending value of z_1/L implies increasing thickness of the upper layer together with decreasing thickness of the lower layer. In Figs. 7 and 8, the values of z_1/L has been varied in the range of $0 < z_1/L < 1$.

When the upper soil layer has negligibly less thickness, i.e., the value of z_1/L is close to zero, majority of the uplift pile capacity is contributed by the lower soil layer. Hence, gradual increase in the thickness of upper layer associated with decreased thickness of the lower layer initiates an initial reduction in uplift pile capacity. For higher values of z_1/L, the upper layer contributes to majority of the uplift pile capacity, initiating in progressive increase in capacity with ascending z1/L. Similar observation was found in few earlier studies as well (Basack and Khabbaz 2024, Yang and Jeremic 2006). Simultaneously, the L/D ratio as well influences the uplift capacity significantly (Mitchell 2005).

The magnitude of ρ_h depends upon the strengths and stiffnesses of both the soil layers, while their relative values

Table 4 Input data for design illustration

Material	Parameter		Value: Layer 1: Sand	Value: Layer 2: Clay
Soil	Bulk unit weight (kN/m^3)		18	15
	Initial shear modulus of soil, G_t^0 (MPa)		0	2.5
	Rate of increase of shear modulus with depth, η_g (MPa/m)		8	0.25 [a]
	Poisson's ratio, v_s		0.3	0.5
	Undrained cohesion at ground surface, c_u^{z1} (kPa)		0	25
	Rate of increase of cohesion with depth, η_c (kPa/m)		0	2.5 [a]
	Adhesion factor, α		-	0.8 [a]
	Effective friction angle, ϕ' (°)		45	0
	Interface friction angle, δ_s (°)		1.0 ϕ' [b]	-
	Lateral earth pressure coefficient, K_s		1-sin ϕ' [b]	-
	Stress reduction factor, R_f		0.9 [c]	0.9 [c]
	Depth below ground surface (m)		6	-
Pile	Diameter	Outer, D (m)	0.5 *	
		Inner, D_i (m)	0 *	
	Embedded length, L (m)		10 *	
	Unit weight of pile material, γ_p (kN/m^3)		25 [d]	
	Young's modulus, E_p (GPa)		3 [d]	
	Plastic stress in tension, σ_p^u (MPa)		500 [e]	

Data assumed after: [a]Basack and Khabbaz (2014), [b]Awad-Alla *et al.* (2009), Kulhawy *et al*. (1983), Kulhawy (1991), [c]Randolph (2003), [d]McCormac and Brown (2015), [e] Moghadam and Izadifard (2021);
* Arbitrarily assumed.Note: Groundwater table is assumed at ground surface

largely influence the pattern of variation of ρ_h (Basack and Khabbaz 2024, Yang and Zhou 2008). As per Eq. (16), the magnitude of ρ_h depends not only upon the uplift pile capacity but also upon the shear modulus of soil at pile base and mid-depth, apart from the peak values of interface shear strength. In case of clay overlying sand, the ascending value of z_1/L from 0 to 1 produced increase initial decrease in the normalized upward pile head displacement (ρ_h/D), followed by progressive increase for higher values of z_1/L , as observed in Fig. 9. The ascending z_1/L produced a variation pattern of ρ_h similar to that of P_u, which may be justified by the possible fact that the magnitude of P_u has predominant influence on ρ_h compared to the magnitudes of ρ_2 and ρ_3 (see Eqs. (18)-(20)).

In case of sand overlying clay, the value of ρ_h/D increased fairly linearly with ascending z_1/L, as visualized from Fig. 10. With the given soil parameters and pile geometry, the component ρ_2 was found to be predominant during computation, compared to the other components ρ_1 and ρ_3. Since ρ_2 is a linear function of z_1 as per Eq. (22), the observed pattern of variation is justified.

Similar findings were observed in few earlier studies as well (Basack and Khabbaz 2024, Basack and Nimbalkar 2018).

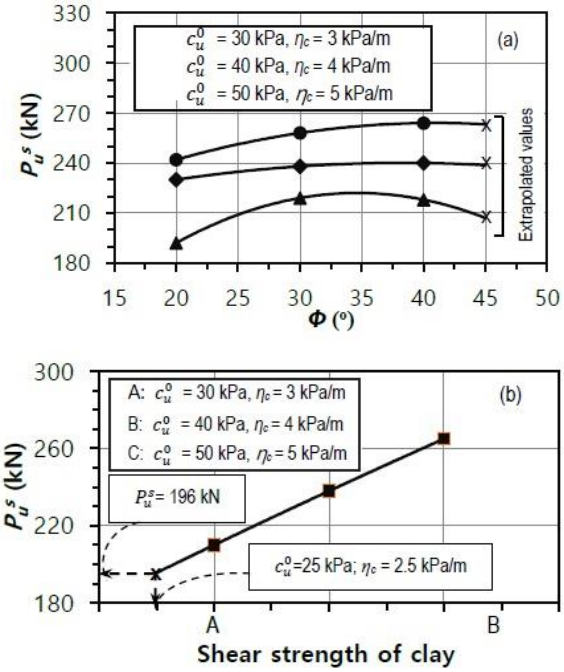

Fig. 11 Graphical estimation of P_u^s : (a) Extrapolated values at ϕ' = 45°, and (b) Evaluation at c_u^0=25 kPa; η_c = 2.5 kPa/m

Table 5 Estimated values of P_u^s

ϕ'(°)	c_u^0 (kPa), η_c (kPa/m)	P_u^s (kN)	ρ_h (mm)
20	30, 3	192	39
	40, 4	230	38.5
	50, 5	242	38
30	30, 3	219	41
	40, 4	238	40.5
	50, 5	258	40.3
40	30, 3	218	41.5
	40, 4	240	41
	50, 5	264	40.5

5.4 Design illustration

To illustrate the use of the methodology and design curves described above, a typical design example has been presented here.

Banu *et al.* (2024) conducted a numerical study on bearing capacity of foundation in a two-layered sand-over-clay subsoil deposit. The soil data of this study has been utilized to evaluate the limit-state uplift performance of an assumed concrete pile embedded in the layered soil. The soil and pile data adopted herein is presented in Table 4.

Since the above data is for sand overlying clay, the design curves in Figs. 8 and 10 shall be considered to estimate the values of P_u and ρ_h. First of all, the value of P_u^p has been evaluated from Eq. (5) as 98174 kN. Using Fig. 8 and 10, the values of P_u^s and ρ_h corresponding to the given

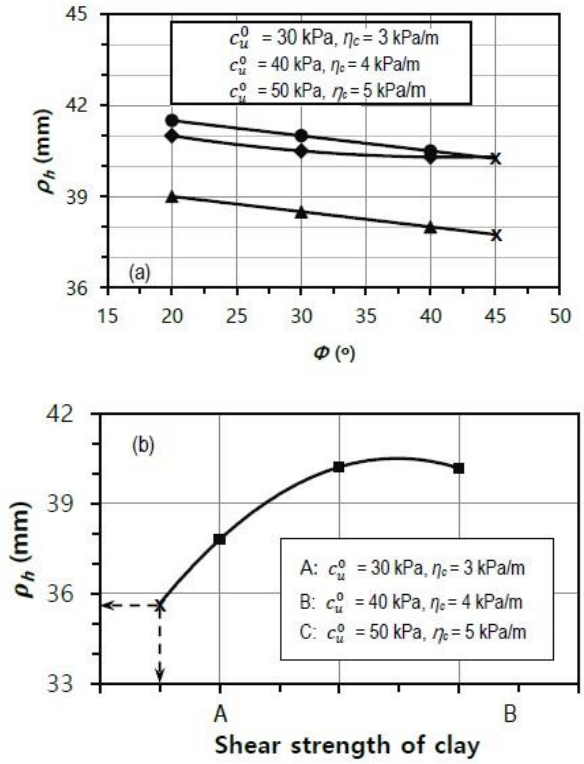

Fig. 12 Graphical estimation of ρ_h: (a) (a) Extrapolated values at ϕ' = 45°, and (b) Evaluation at c_u^0=25 kPa; η_c = 2.5 kPa/m

L/D = 20 has been estimated for different values of ϕ', c_u^0 and η_c, as presented in Table 5.

The values of P_u^s from Table 5 have been plotted against the values of ϕ' for different values of c_u^0 and η_c (see Fig. 11(a)) and the curves are extrapolated to estimate the magnitudes of P_u^s for ϕ' = 45°. These extrapolated values have been plotted against different values of c_u^0 and η_c (see Fig. 11(b)) and once again extrapolated to estimate the magnitudes of P_u^s corresponding to the given values of c_u^0 and η_c as per Table 5. As found, the magnitudes of P_u^s for z_1/L = 0.6 have been evaluated as 196 kN against the analytically derived value from Eq. (9) as 217 kN, with a deviation below 10%.

Similarly, the value of ρ_h has been estimated as 35.7 mm, using graphical extrapolation technique shown in Fig 12. From Eqs. (17), (18), (22) and (23), the analytical value of ρ_h has been evaluated as 40.1 mm. The deviation is thus below 11%.

6. Significance and limitations

Several theoretical and experimental investigations on piles under uplift load has already been conducted, although rigorous mathematical analysis on the limit state performance of tension piles in layered soil have been inadequate. The solution presented here is based on rigorous mathematical analysis for limit state uplift performance of single pile in two-layered soil. In order to verify the accuracy of the correlations developed, the analytical results have been compared with available in-situ test data, wherein a reasonably good agreement is observed. The model has further been utilized to develop a series of graphical representations on the variation of ultimate uplift capacity and limiting upward pile displacement with soil layer thickness ratio, for different pile geometry and soil strengths and stiffnesses. These curves may be utilized to design the piles in specified soil and pile parameters.

- The analytical model has following inherent limitations: The specific installation techniques impart residual stresses on soil (Reda *et al.* 2023), but the model is unable to capture the influence of pile installation.
- The analysis is applicable whenever the layers are pure cohesive or granular soil. For *c*-ϕ soil, the further analysis with modification of the correlations might be required (e.g., Dehghanbanadaki *et al.* 2021).
- In case of socketed pile, the base is restrained against upward displacement (Poulos and Davis 1980). The model is not applicable to such condition.

7. Conclusions

In spite of several past studies on uplift piles, analysis of piles under pullout load in layered soil is insufficient. Employing the limit state analysis, a mathematical model has been developed to derive the ultimate uplift capacity and peak upward pile head displacement of single pile in two layered soils. Comparison of the analytical results derived from the current model with field tests data from the past studies implied reasonable accuracy of the formulations developed.

The study revealed that the normalized ultimate uplift pile capacity varied in curvilinear patterns with ascending slopes with respect to the soil layer thickness ratio z_1/L. In case of clay overlying sand, the normalized capacity $P_u/(\alpha c_u^0 D^2)$ varied in the range of 36-225 for the chosen soil and pile parameters. In case of sand overlying clay, on the other hand, the normalized pile capacity $P_u/(\alpha K_s \tan\delta_s \gamma_s' D^3)$ varied from 2.5 x 10^3 to 50 x 10^3. In both the cases, the magnitudes of normalized capacity initially decreased with ascending values of z_1/L, and thereafter increased gradually. The value of z_1/L at which the minimum capacity attained was found to increase progressively with ascending shear strength of soil layers.

The normalized peak upward pile head displacement ρ_h/D was observed to vary with z_1/L. The magnitudes of peak displacement progressively decreased with increasing soil strength and stiffness. In case of clay overlying sand, the pattern of variation was curvilinear with ascending slope. With the chosen soil and pile parameters, the magnitude of ρ_h/D varied in the range of 1% - 2.2%. With ascending value of z_1/L, the peak displacement initially reduced and thereafter increased, for L/D ratio of 20 and 30, the minimum magnitude being occurring at z_1/L = 0.75 and 0.85, respectively. In case of sand overlying clay, on the other hand, the pattern of variation was found to be almost linearly increasing, with the magnitudes varying from 0.38% to 1.35% for the chosen soil and pile parameters.

Acknowledgments

The authors extend their appreciation to the Deanship of Research and Graduate Studies at King Khalid University for funding this work through Large Research Project under grant number RGP2/57/46. The infrastructural supports received from Regent Education and Research Foundation and the Civil Engineering Department of Graphic Era Deemed to be University are also acknowledged.

References

Alawneh, A. (1999), "Tension piles in sand: a method including degradation of shaft friction during pile driving", *Transport. Res. Record*, **1663**(1), 41-49. https://doi.org/10.3141/1663-06.

Anbazhagan, P., Aditya, P. and Rashmi, H.N. (2012), "Review of correlations between SPT N and shear modulus: A new correlation applicable to any region", *Soil Dyn. Earthq. Eng.*, **36**, 52-69.

Anbazhagan, P., Kumar, A. Ingale, S.G., Jha, S.K. and Lenin, K.R. (2021), "Shear modulus from SPT N-values with different energy values", *Soil Dyn. Earthq. Eng.*, **150**(106925), https://doi.org/10.1016/j.soildyn.2021.106925.

Ashour, M. and Abbads, A. (2020), "Response of piles in multilayers of soil under uplift forces", *Int. J. Geomech.*, **20**(6). https://doi.org/10.1061/(ASCE)GM.1943-5622.0001676.

Awad-Alla, F., Yasufuku, N. and Omine, K. (2009), "Evaluation of accuracy and predictability of the methods used for calculating ultimate horizontal load of piles", *J. Egyptian Geotech. Soc.*, **20**(2), 213-228.

Banu, S., Attom, M., Abed, F., Vandanapu, R., Astillo, P.V., Al-Lozi, N. and Khalil, A. (2024), "Numerical analysis of the ultimate bearing capacity of strip footing constructed on sand-over-clay sediment", *Buildings*, **14**(4), 1164. https://doi.org/10.3390/buildings14041164.

Basack, S., Alkahtani, M.Q. and Islam, S. (2025), "Single pile response to uplift load: computational model and analysis", *Mar. Georesour. Geotech.*, https://doi.org/10.1080/1064119X.2024.2448734.

Basack, S. and Khabbaz, H. (2024), "Analytical solution for single pile in two-layered soil subjected to torsion", *Geomech. Geoeng*., https://doi.org/10.1080/17486025.2024.2433203.

Basack, S. and Nimbalkar, S. (2017), "Numerical solution of single pile subjected to torsional cyclic load", *Int. J. Geomech.*, **17**(8), https://doi.org/10.1061/(ASCE)GM.1943-5622.0000905.

Basack, S. and Nimbalkar, S. (2018), "Measured and predicted response of pile groups in soft clay subjected to cyclic lateral loading", *Int. J. Geomech.*, **18**(7), https://doi.org/10.1061/(ASCE)GM.1943-5622.0001188.

Basack, S. and Sen, S. (2014), "Numerical solution of single piles subjected to pure torsion", *J. Geotech. Geoenviron. Eng.*, **140**(1). https://doi.org/10.1061/(ASCE)GT.1943-5606.0000964.

Basack, S., Karami, M. and Karakouzian, M. (2022), "Pile-soil interaction under cyclic lateral load in loose sand: Experimental and numerical evaluations", *Soil Dyn. Earthq. Eng.*, **162**(107439), https://doi.org/10.1016/j.soildyn.2022.107439.

Bertram, A. and Glüge, R. (2015), "Solid mechanics: Theory, modeling and problems", Springer International Publishing, Switzerland. https://doi.org/10.1007/978-3-319-19566-7.

Carvalho, D.D. and Albuquerque, R.D. (2013), "Uplift behavior of bored piles in tropical unsaturated sandy soil", *Proceedings of the 18th International Conference on Soil Mechanics and Geotechnical Engineering*, Paris, France.

Cherubini, C. and Vessia, G. (2007), "Reliability approach for the side resistance of piles by means of the total stress analysis (α Method)", *Can. Geotech. J.*, **44**, 1378-1390. https://doi.org/10.1139/T07-061.

Das, B.M. and Seeley, G.R. (1982), "Uplift capacity of pipe piles in saturated clay", *Soils Found.*, **22**(1), 91-94. https://doi.org/10.3208/sandf1972.22.91.

Dehghanbanadaki, A., Khari, M., Amiri, S.T. and Armaghani, D.J. (2021), "Estimation of ultimate bearing capacity of driven piles in c-φ soil using MLP-GWO and ANFIS-GWO models: A comparative study", *Soft Comput.*, **25**, 4103-4119. https://doi.org/10.1007/s00500-020-05435-0.

Dong, C., Yu, G. and Gong, Y. (2023), "Experimental study on pull-out behaviour of piles in cohesive sedimentary beds subject to water jet and vibration loading", *Appl. Ocean Res.*, **141**(103787). https://doi.org/10.1016/j.apor.2023.103787.

Fang, J., Lin, S. and Liu, K. (2023), "Multi-scale study of load-bearing mechanism of uplift piles based on model tests and numerical simulations", *Scientific Reports*, **13**, 6410. https://doi.org/10.1038/s41598-023-33221-z.

Federal Highway Administration (2006), "*Analyses of the Axial Load Tests at the Route 351 Bridge*", Chapter 7, Federal Highway Administration Research and Technology, U.S. Department of Transportation, Washington DC, USA, https://www.fhwa.dot.gov/publications/research/infrastructure/structures/04043/07.cfm

Gui, F., Kong, J., Feng, D., Qu, X., Zhu, F. and You, Y. (2021), "Uplift resistance capacity of anchor piles used in marine aquaculture", *Scientific Reports*, **11**(20321). https://doi.org/10.1038/s41598-021-99817-5

Hong-nan, H., Guo-liang, D. and Wei-ming, G. (2015), "Review of computational models and methods for predicting ultimate capacity of uplift piles with uniform cross section", *J. Highway Transport. Res. Development*, **9**(2). https://doi.org/10.1061/JHTRCQ.0000443.

Karami, M., Basack, S., Das, G., Bhadra, D. and Karakouzian, M. (2023), "Experimental and numerical evaluations of load settlement response of helical piles in soft clay", *Mar. Georesour. Geotech.*, **42**(9), 1146-1163.

Karami, M., Basack, S., Pan, M., Das, G., Gupta, A. and Karakouzian, M. (2024), "Experimental and numerical investigations on the performance of screw micropiles under pull-out and lateral loads", *Int. J. Geotech. Eng.*, 1-23.

Kranthikumar, A., Sawant, V.A. and Shukla, S.K. (2016), "Numerical modeling of granular anchor pile system in loose sandy soil subjected to uplift loading", *Int. J. Geosynth. Ground Eng.*, **2**(15). https://doi.org/10.1007/s40891-016-0056-4.

Kulhawy, F.H., Trautmann, C.H., Beech, J.F., O'Rourke, T.D., McGuire, W., Wood, W.A. and Capano, C. (1983), "Transmission line structure foundations for uplift-compression loading", Rep. No. EL-2870, Electric Power Research Institute, Palo Alto, Calif.

Kulhawy, F.H. (1991), "Drilled shaft foundations, foundation engineering handbook", 2nd Ed., Chap. 14, (Ed., H.Y. Fang), Van Nostrand Reinhold, New York.

Kumar, M.P., Raju, P.M., Jasmine, G.V. and Aditya, M. (2020), "Settlement analysis of pile cap with normal and under-reamed piles", *Geomech. Eng.*, **25**(6), 525-535. https://doi.org/10.12989/cac.2020.25.6.525.

Lee, J., Kim, M. and Lee, S.H. (2009), "Reliability analysis and evaluation of LRFD resistance factors for CPT-based design of driven piles", *Geomech. Eng.*, **1**(1), 17-34. https://doi.org/10.12989/gae.2009.1.1.017.

Li, G., Zhang, J., Liu, J. and Li, J. (2021), "Study on the Uplift Bearing Capacity of Rock-Socketed Piles", *Soil Mech. Found. Eng.*, 203-208. https://doi.org/10.1007/s11204-021-09729-9.

Liu, C., Ji, F., Song, Y., Wang, H., Li, J., Xuan, Z. and Zhao, M. (2023), "Upper bound analysis of ultimate pullout capacity for a single pile using hoek–brown failure criterion", *Buildings*,

13(12), 2904. https://doi.org/10.3390/ buildings13122904.

Massoudi, N. and Bell, K.R. (2017), "Load testing and performance of instrumented ACIP piles in Texas clays", *Proceedings of the Geotechnical Frontiers*, Orlando, Florida, USA. https://ascelibrary.org/doi/10.1061/9780784480465.038.

McCormac, J.C. and Brown, R.H. (2015), "*Design of Reinforced Concrete*", 10th Edition, Wiley Publication, 87910-8, 672.

Mitchell, P.W. (2005), "Bearing capacity of jacked piles in a layered soil profile", *Aust. Geomech. J.*, **40**(2). https://australiangeomechanics.org/journals/.

Moghadam, M.A. and Izadifard, R.A. (2021), "Prediction of the tensile strength of normal and steel fiber reinforced concrete exposed to high temperatures", *Int. J. Concrete Struct. Mater.*, **15**(47). https://doi.org/10.1186/s40069-021-00485-6.

Narasimha Rao, S. and Prasad, Y.V.S.N. (1993), "Estimation of uplift capacity of helical anchors in clays", *J. Geotech. Eng.*, **119**(2), https://doi.org/10.1061/(ASCE)0733-9410(1993)119:2(352).

Nour El-Deen, A., Shahien, M., Mansour, M. and Rabie, M. (2025), "Enhancing pullout capacity of single piles and pile groups using geosynthetic soil-reinforcement technique", *Eng. Res. J.*, **184**(2), 178-196. https://doi.org/10.21608/erj.2025.344539.1163.

Park, S.H. and Lee, J.K. (2021), "Ultimate uplift resistance of circular plate anchors in undrained two-layer clays", *Geomnech. Eng.*, **27**(3), 213-221. https://doi.org/10.12989/gae.2021.27.3.213.

Phanikanth, V.S., Choudhury, D. and Reddy, R. (2010). "Response of single pile under lateral loads in cohesionless soils", *Electron. J. Geotech. Eng.*, **15**, 1-18.

Poulos, H.G. and Davis, E.H. (1980), "Pile foundation analysis and design", John Wiley & Sons, New York, USA.

Pusadkar, S.S. and Ghormode, S.N. (2015), "Uplift capacity of piles in two-layered soil", *Int. J. Civil Eng. Technol.*, **6**(3), 132-138.

Raju, K.V.S.B. and Lakshmi, V. (2025), "Pullout and oblique pullout resistance of enlarged base piles in geogrid reinforced sand", *Geo-Eng.*, **16**, 12. https://doi.org/10.1186/s40703-025-00239-3.

Randolph, M.F. (2003), "Load transfer analysis of axially loaded piles", Technical Report, Centre for Offshore Foundation Systems, University of Western Australia, Perth, Australia.

Randolph, M.F. and Wroth, C.P. (1978), "Analysis of deformation of vertically loaded piles", *J. Geot. Eng. Div. ASCE*, **104**(12), 1465-1488.

Reda, A., Amaechi, C.V. and Shahin, M.A. (2023), "Case study for effects of pile installation on existing offshore facilities in brownfields", *Appl. Ocean Res.*, **138**(103651). https://doi.org/10.1016/j.apor.2023.103651.

Reddy, M.K. and Ayothiraman, R. (2015), "Experimental studies on behavior of single pile under combined uplift and lateral loading", *J. Geotech. Geoenviron. Eng.*, **141**(7), https://doi.org/10.1061/(ASCE)GT.1943-5606.0001314.

Saleh, H.M., Jebur, M.M., Mohammed, M.Q., Karkush, M. and Sabri, M.M. (2025), "Numerical investigation of pullout capacity of under-reamed piles in clayey soils", *Front. Built Environ.*, **11**. https://doi.org/10.3389/fbuil.2025.1582340.

Su, Q., Zhang, X., Yin, P. and Zhao, W. (2014), "Ultimate capacity analysis and determination of the position of failure surface for uplift piles", *Math. Probl. Eng.*, http://dx.doi.org/10.1155/2014/540143.

Wang, L. (2022), "Dynamic response of pile group in two-layered soils under scour condition by FEM-ALEM approach", *Appl. Math. Model.*, **112**, 341-357. https://doi.org/10.1016/j.apm.2022.07.037.

Xu, H.Y., Chen, L.Z. and Deng, J.L. (2014), "Uplift tests of jet mixing anchor pile", *Soils Found.*, **54**(2), 168-175. https://doi.org/10.1016/j.sandf.2014.02.008.

Yang, Z. and Jeremic B. (2006), "Study of soil layering effects on lateral loading behavior of piles", *J. Geotech. Geoenviron. Eng.*, **131**(6). https://ascelibrary.org/doi/abs/10.1061/(ASCE)1090-0241(2005).

Yang, X. and Zou, J. (2008), "Displacement and deformation analysis for uplift piles", *J. Cent. South Univ. Technol.*, 15, 906-910. https://doi.org/10.1007/s11771-008-0165-x.

Yu, Y.C., Ren, W.X., Yin, Y.G. and Luo, X.G. (2023), "Numerical simulation and field tests on vertical load bearing behaviour of bored root piles", *Comput. Geotech.*, 159(105453). https://doi.org/10.1016/j.compgeo.2023.105453.

Zhang, Q.Q., Feng, R.F., Liu, S.W. and Li, X.M. (2018), "Estimation of uplift capacity of a single pile embedded in sand considering arching effect", *Int. J. Geomech.*, **18**(9). https://doi.org/10.1061/(ASCE) GM.1943- 5622.0001240.

Zhu, H.H., Mei, G.X., Xu, M., Liu, Y. and Yin, J.H. (2014), "Experimental and numerical investigation of uplift behavior of umbrella-shaped ground anchor", *Geomech. Eng.*, **7**(2), 165-181. https://doi.org/10.12989/ gae.2014.7.2.165.

CG